Journal of Sol-Gel Science and Technology, 5, 173–183 (1995)
© 1995 Kluwer Academic Publishers, Boston. Manufactured in The Netherlands.

Spin Coating Process of Sol-Gel Silicate Films Deposition: Effect of Spin Speed and Processing Temperature

KONSTANTIN VOROTILOV, VLADIMIR PETROVSKY AND VLADIMIR VASILJEV
Moscow Institute of Radioengineering, Electronics and Automation, Vernadsky prosp., 78, 117454—Moscow, Russia

Received August 19, 1993; Accepted June 22, 1995

Abstract. The effect of two factors having the most important influence on spin coating process of sol-gel films: the spin speed and the temperature (of the substrate and the applied solution) during film deposition is discussed. It is shown, that film thickness and thickness uniformity are determined by centrifugal driving force dynamics, viscous polymer rheology, solvent evaporation dynamics, and film porous microstructure.

Keywords: sol-gel film, spin coating process, spin speed, processing temperature

1 Introduction

Thin films and coatings were the earliest and remain so far one of the most important applications of sol-gel technology [1, 2]. Recent years are marked by growing interest in sol-gel processed films in new areas, in particular in microelectronics. This is mainly due to intensively developing applications of silicate or siloxane sol-gel films in the VLSI multilevel interconnection process, preparation of ferroelectric films for nonvolatile memory and so on (see e.g., [3–5]). The distinguishing features needed in applications for the microelectronics industry are very high requirements on films quality (including electric and mechanic properties, uniformity, low particles and microadmixtures contamination, high reproducibility and so on). Therefore the wide practical application of the sol-gel techniques in such areas as microelectronics calls for detailed information on physical and chemical aspects of the sol-gel film formation process.

Spin coating is the main technique for film deposition from liquid precursors used in the microelectronics industry. A large variety of high-performance systems, providing coatings of photoresists, polyimides and spin-on-glasses (SOG) are available from manufacturers. Other deposition techniques are practically not used in semiconductor production. Thus dipping is frequently used in sol-gel film preparation, it has a number of limitations: double side coating, nonuniformity on wafer edge, rather high contamination level (solution is polluted by the particles from the wafer and the container walls which are then recoated from the solution surface into the growing film; the solution applied cannot be filtered just before use) and some others. New advanced meniscus coating technique is practically free from most of these limitations, but it is more appropriate for the present for right-angled samples of a rather large size [6]. Other techniques such as spray pyrolysys also do not provide necessary uniformity and low contamination level. It seems considerably promising applying the new technique of LSCVD (liquid source chemical vapor deposition) recently developed by Symetrix Corporation [7] and that consists of spraying of sol-gel precursors in vacuum under high precision control. But the future of this technique depends on progress in construction and application in industry of rather complex and expensive equipment. Therefore the practical application of sol-gel thin film route at least for microelectronic applications is connected with the spin coating process.

The most part of investigations in the field of sol-gel thin films deals with the effect of composition and polymolecular structure of initial sol as well as annealing conditions on the film properties, whereas deposition conditions may strongly influence the thickness, porous microstructure, and other properties of the formed layers. Brinker et al. [1, 8], Strawbrige and James [9] and some others have performed detailed investigation on physical and chemical aspects of film application by dipping. Unfortunately, spin coating of sol-gel films is less-well investigated.

Bornside et al. [10] distinguish the following basic steps of the spin coating process: deposition, spin-up, spin-off and evaporation. During the first two stages

an excess of the liquid is dispensed onto a wafer and spreads out due to spinning-indused forces with usually a low initial rate (hundreds of revolutions per minute (rpm)). At the spin-off stage spin speed increases (up to thousands of rpm) and the liquid flows radially under centrifugal force. Film thinning by centrifugally driven convective outflow decreases with time as convective outflow is proportional to film cubic thickness for a newtonian liquid [11] and becomes comparable to the rate of film thinning by solvent evaporation. The viscosity is drastically increased and the centrifugally driven convective outflow is ceased. At the last stage, film thinning occurs only due to solvent evaporation.

The mathematical description of the spin coating process is a relatively complex matter. The examination of the spin coating process includes the centrifugal driving force dynamics, viscous polymer rheology, and solvent evaporation dynamics. The change in diffusivity, viscosity and rheology during film formation complicates the issue. Since the end of the 1950s, a series of mathematical models considered spin coating on a flat substrate (see e.g., [10–21]) and recently those dealing a substrate with a topographic features (see e.g., [22–24]) have been published. These models give insight into the influence of physical properties of the applied liquid (such as concentration, viscosity etc.) and deposition conditions (mainly the spin speed) on the film thickness and the film uniformity. The numerical solution of a system of differential equations by computer are used to predict the film thickness.

A simplified model of the spin-coating process predicting dry film thickness as a function of a number of physical parameters was proposed by Meyerhofer [13] and advanced by Bornside et al. [20]. The model assumes that the spin-off and evaporation stages are sequential and uncoupled (no evaporation at the spin-off stage, only centrifugally driven convective outflow occur). The resulting expression for the solid film thickness h_s is [20–21]:

$$h_s = (1 - x_0)\left[\left[\frac{3\eta_1^0}{2\rho_1^2\omega^2}\right]\frac{p^* M}{R_g T} k x_0\right]^{1/3}, \quad (1)$$

where x_0 is the initial concentration of solvent, η_1^0 and ρ_1 are the viscosity and the density of the liquid; p^*, M are the vapor pressure and the molecular weight of the pure solvent; R_g is the ideal gas constant; T is the temperature; k is the mass transfer coefficient:

$$k = cD(\omega/\nu)^{1/2}, \quad (2)$$

where c is the constant that depends on the Schmidt number (estimated by Bornside et al. [21] $k = 1.74$ cm/s at $\omega = 2000$ rpm); D is the binary diffusivity of the solvent in air; ν is the kinematic viscosity of the overlying gas.

From Eq. (1) $h_s \propto \omega^{-1/2}$. Experimental studies of spin coating of photoresists, polyimides, etc., show the spin speed dependence $h_s \propto \omega^{-\lambda}$, where λ varies from 0.45 to 1.4 (for some polyimides), but more frequently reported values are near $\lambda = 0.5$. Theoretical modeling shows that deviation from the exponent $\lambda = 0.5$ may be connected with the evaporation characteristics of the material [19] or with the non-newtonian rheology of the fluid (e.g., viscosity versus shear rate dependence) (see e.g., [14, 18, 19]).

Emslie, Bonner, and Peck [11] in their pioneering work showed that the spin coating with nonevaporating, newtonian liquid leads to a uniform film by any initial nonuniform distribution. But the inclusion of non-newtonian rheology shows that under certain conditions nonuniform films may be formed (the film thickness is the most prominent at the film center and decreases towards the wafer edge) [12, 15, 19]. Recently Bornside et al. [21] have demonstrated the important role of air flow dynamics during the spin coating. The turbulent flow at the periphery of the spinning disk may produce an increase of mass transfer coefficient leading to increase of film thickness at the wafer edge.

Experimental studies of the spin coating process have been performed mainly for photoresists and polyimides. Physical and chemical processes of spin coating of sol-gel films have special features. The effect of two factors having a dramatic impact on spin coating process of sol-gel films: the spin speed and the temperature (of the substrate and the solution) during film deposition is discussed in this work.

2 Spin Coating Process of Sol-Gel Films

The sol-gel process has some peculiarities which have to take into account on examination of spin coating. The transition of initial liquid sol to solid-like gel occurs as a result of proceedings of polycondensation reaction with progressive branching of metal-oxide network. The microstructure of a porous gel obtained after spin coating transforms further at drying and annealing, during which the resulted microstructure of the film depends not only on initial gel structure but also on drying conditions. Thus for real film thickness of

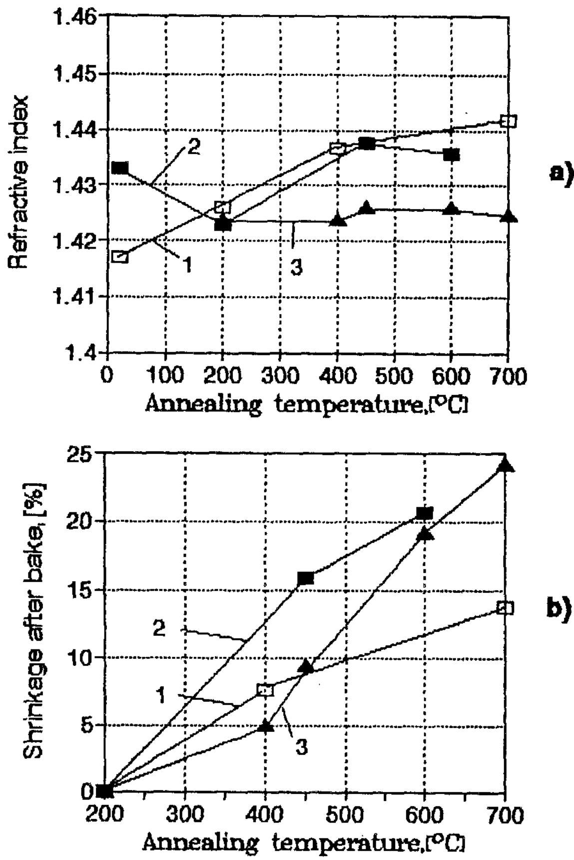

Fig. 1. The dependence of the refractive index (a) and the shrinkage (b) of sol-gel silicate films as a function of the heat treatment: 1—the data of this study (see Section 4); 2-[26]; 3-[27].

sol-gel film h_f the film porosity must take into account in Eq. (1):

$$h_f = h_s / V_s, \tag{3}$$

where V_s is the volume fraction solids.

Brinker et al. [1, 25] propose to use the refractive index to estimation of pore volumes of the films as it follows from the Lorentz-Lorenz relationship:

$$\left(n_f^2 - 1\right) / \left(n_f^2 + 2\right) = V_S\left(n_S^2 - 1\right) / \left(n_S^2 + 2\right), \tag{4}$$

where n_f is the film refractive index, V_S is the volume fraction of solids, and n_S is the refractive index of the solid skeleton.

For small variations in the refractive index the volume fraction of solids may be expressed as:

$$V_S = 1 - \frac{6n_s(n_s - n_f)}{\left(n_S^2 - 1\right)\left(n_S^2 + 2\right)}. \tag{5}$$

In the case of silica films ($n_s = 1.458$):

$$V_S = 1 - 1.883(1.458 - n_f). \tag{6}$$

To test this suggestion let us consider the typical data on evolution of the refractive index and the shrinkage during the heat treatment of sol-gel silicate films (see Fig. 1 [26, 27]). Although in some cases the refractive index shows slight increase with the heat treatment temperature, the variations in the refractive index are insignificant in contrast to the film shrinkage. Thus it can be obtained from Eq. (6) that the 10% shrinkage of porous film must cause 0.053 increase in the refractive index. The reason of this inconsistency is a high hydroxyl content that has grater impact on the refractive index of sol-gel silicate films than their porosity.

By this means the refractive index of sol-gel silicate films cannot be strictly considered as characteristic of the film porosity and direct techniques of porosity measurement are needed (e.g., Brinker et al. have proposed N_2 adsorption-desorption technique with the use of surface acoustic waves [25]). Unfortunately, the measurements of the film's porosity have not been done in this work because of sophistication of such techniques.

3 Spin Speed Dependence and Radial Uniformity

3.1 Experimental Procedures

Silica precursor solutions were prepared by mixing tetraethoxysilane with absolute n-butanol, deionized water and HCl. The equivalent oxide concentration was 6% and [alkoxide] : [H_2O] : [HCl] = 1 : 7 : 0.04. After stirring the solution was kept for 24 h at 60°C. Before the deposition procedure the solution was filtered through a 0.2 μm filter.

Silicon wafers with 100.2 mm diam were used as substrates. Wafers was cleaned before use by:

(i) $H_2SO_4 : H_2O$ (3 : 2) solution at 140°C during 10 min;
(ii) rinsing in deionized water;
(iii) $H_2O_2 : NH_4OH : H_2O$ (1 : 1 : 5) mixture at 65°C for 10 min;
(iv) rinsing in deionized water.

The spin coating was performed at room temperature using a photoresist spinner (Lada-125, Voronezh, Russia). The coating solution doses (1 ml) were dispensed onto the center of the stationary wafer (no special programmed path over the wafer was used) which was then spun at a speed of 500 rpm for 4 s, and after

Table 1.

Spin speed, RPM	Thickness, A		Refractive index		Nonuniformity, %
	Center	Edge	Center	Edge	
500	3147	3000	1.396	1.430	4.67
1000	1968	1892	1.444	1.445	3.86
2000	1311	1262	1.430	1.434	3.74
3000	1079	1048	1.437	1.432	2.87
4000	878	859	1.426	1.430	2.16

this, the spin speed was increased up to 4000 rpm for 40 s. After film depositions the wafers were dried at $T_a = 200°C$ for 30 min in N_2.

The film thicknesses and refractive indexes were measured in 10 points at intervals of 5 mm from the wafer center by multiangle ellipsometry at the 6328 Å wavelength and the incident irradiation angles from 45 to 70° [28]. The real and imaginary parts of the refractive index of the uncoated silicon substrate was determined to be 3.85 and −0.02, respectively.

3.2 *Spin Speed Dependence*

The film thickness h_f and the refractive index n_f measured at the center and the edge of the substrate (after drying at $T_a = 200°C$), as well as the percentage nonuniformity (from the center to the edge) of silicate sol-gel films prepared with the different spin speeds are presented in Table 1.

The film thickness h_f and the refractive index n_f measured at the center and the edge of the substrate (after drying at $T_a = 200°C$), as well as the percentage nonuniformity (from the center to the edge) of silicate sol-gel films prepared with the different spin speeds.

Approximation of the data for film thickness gives $h_f = 1294889 \cdot \omega^{-0.60}$ in the center, and $h_f = 115034 \cdot \omega^{-0.59}$ in the edge. The slopes of these dependences ($\lambda = -0.59 \cdots -0.60$) somewhat differ from the limited available published data for the same types of films. Thus, Wu [29] reported $\lambda \approx 0.5$ for the spin-on arsenic glasses. Some data for spin-on glasses (SOGs) obtained from Allied Chemical Corporation were collected by Sukanek [19]. He reported $\lambda = 0.45 - 0.58$ for various SOGs with unknown compositions (silicates and siloxanes). The best fit line for this data have the slope $\lambda = 0.476$.

Unfortunately, both our experiment and the published results have no data concerning film porosity which has to be taken into account in accordance with Eq. (3). The refractive index of silicate films is changed very slightly with the spin speed (see Table 1) and as it was discussed in Section 2 it does not determine film porosity adequately because of hydroxyl content. Although we do not know the contribution of the film porosity in λ some other reasons for increase of λ from the value $\lambda = 0.5$ predicted by the Meyerhofer's approximation (Eq. (1)) are worth consideration.

The first lies in the solvent evaporation behaviour. As shown by Sukanek [19] the change of exponent in spin speed dependence of the mass transfer coefficient k causes the corresponding change of λ. If the evaporation rate is independent of the spin speed the $h_f \propto \omega^{-2/3}$; if $k \propto \omega^{1/2}$ (mass transfer from a rotating disk) (Eq. (2)) then $h_f \propto \omega^{-1/2}$ (Eq. (1)); finally, in the case of no evaporation $h_f \propto \omega^{-1}$. The change in evaporation dynamics during spin coating is mainly connected with the formation of a region at the free surface with extremely low solvent concentration and low binary diffusivity (skin layer) [17]. If this layer is formed at the early stages of the spin coating process it will hinder the free solvent evaporation producing a change from $\lambda = 0.5$ towards $\lambda = 1$. Formation of such a skin layer is highly plausible during spin coating of sol-gel films, because in contrast to photoresists, the polycondensation processes proceed very rapidly with the production of a dense glass-like layer. The obtained experimental dependence with $\lambda \cong 0.6$ in the framework of this interpretation suggests the presence of such skin layer.

But there exists an other physical mechanism leading to the same results—non-newtonian rheology of the deposited sol. In this case after reaching the estimated shear rate the liquid viscosity is beginning to decrease (shear-thinning behavior). The critical shear rate, at which the non-newtonian behavior appears, is rather high for diluted polymer solution, and fairly low with concentrated ones. In the sol-gel systems the increase of concentration leads to aggregate growth causing an increase of viscosity, but these aggregates are broken with the shear rate increase and therefore the viscosity falls [1]. The viscosity decrease leads to the increase of convective centrifugally driven outflow and, therefore, to a higher exponent in the dependence $h_f \propto h_0\omega^{-\lambda}$. Thus, Shimoji [18] predicted on the basis of the power-law model $\lambda > 2/3$. It is of value that non-newtonian rheology always leads to radial thickness nonuniformity. Such nonuniformity truly occurs in the films involved and will be discussed below. Sukanek [19] pointed out that the non-newtonian nature of the fluid has no influence on the spin speed dependence of the thickness in the central, uniform region. But there is no

significant difference in the value of λ in the center and in the edge of the wafer. So it may be concluded that there are no sufficient experimental data at this time providing unambiguous indication in favour of one of the discussed models and therefore more detailed investigation is needed.

3.3 Radial Nonuniformity

Film thickness and refractive index profiles for the silicate sol-gel films (after drying at 200°C) obtained at 2000 and 4000 rpm are shown in Fig. 2(a) and (b). The film thickness decreases and the refractive index slightly grows up from the center to the edge indicating on some increase of film density on the edge of the wafer. As in the previous case it is not clear whether the decrease in the film thickness is fully due to film shrinkage (which causes the increase of film density) or not. Anyway to discuss possible reasons of radial nonuniformity let us consider the effects of the air flow dynamics and the non-newtonian liquid rheology.

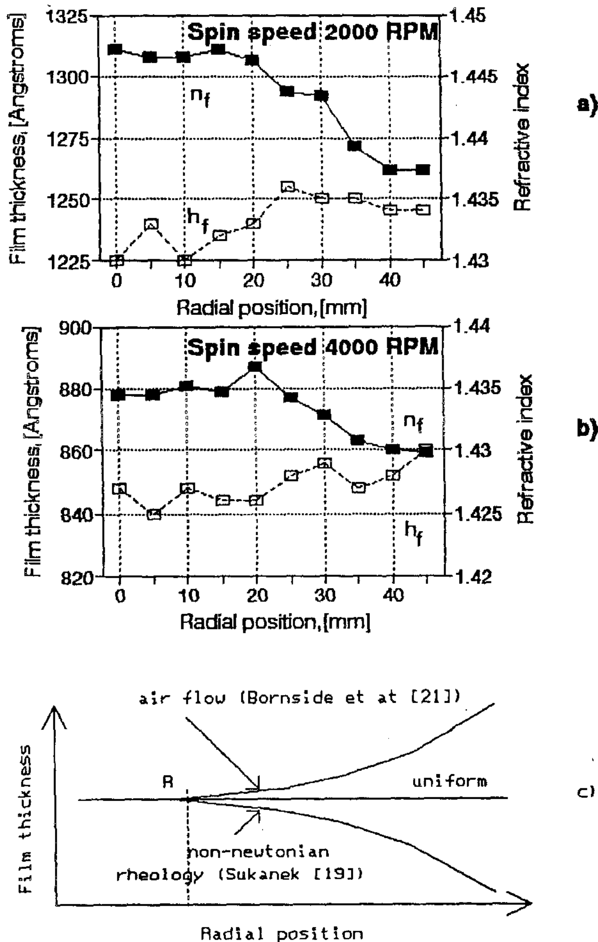

Fig. 2. The film thickness and the refractive index profiles for silicate sol-gel films (after drying at 200°C) prepared at 2000 (a) and 4000 (b) rpm. Possible reasons for variation in thickness with radial position (c): i) hydrodynamic instabilities in the gas flow which lead to nonuniform evaporation from the film during drying and to increase in film thickness towards the wafer edge (D.E. Bornside et al [21]); ii) a non-newtonian nature of the fluid results in thinner film towards the wafer edge (P.C. Sukanek [19]).

Discussing the air flow dynamics, Bornside et al. [21] have distinguished three flow regimes which may be present above a spinning disk: for radii less than some critical value the flow is axisymmetric, laminar, and steady state and the mass transfer coefficient is independent of the radial position; this regime is followed by a transition one, that with three-dimensional spiral vortices, which transforms in its turn into a turbulent flow with a radially dependent mass transfer coefficient. Film thickness must be invariant in this case upto some value of R bounding the region of laminar and steady state air flow. For radial position higher R the mass transfer coefficient will increase, causing the increase of the film thickness on the edges of the wafer (see Eq. (1)). That is why, the discussed mechanism is not responsible for the obtained experimental dependencies.

In contrast to it, the non-newtonian rheology of deposited liquid leads to the opposite radial film thickness profile [19]. In this case, as in the one discussed above, the film remains uniform up to some radial position R corresponding to the critical value of shear rate up to which the liquid viscosity is independent on the shear rate. For higher than R distances from the center reveals the non-newtonian behavior of liquid consisting in the decrease of viscosity with shear rate. It leads to enhanced convective outflow and film thinning towards the wafer edge. Experimental dependences (Fig. 2(a, b)) as a whole are consistent with these assumptions—there is some uniform area after which the film thinning begins. But, in accordance with Sukanek [19], the region of nonuniformity moves toward the center of the wafer with the increase of the spin speed ($R \propto 1/\omega^2$). Moreover, Sukanek has shown [19] that the magnitude of the nonuniformity will increase with the spin speed (the Deborah number characterizing non-newtonian effects $De \propto \omega^{2/3}$) which is in contrast with the experimental data presented in Table 1. The reason of this event to our mind, is that the truncated power law model used by Sukanek [19] does not take into account the dependence of viscosity on concentration. For low spin speed the transfer from spin-off to evaporation stage takes

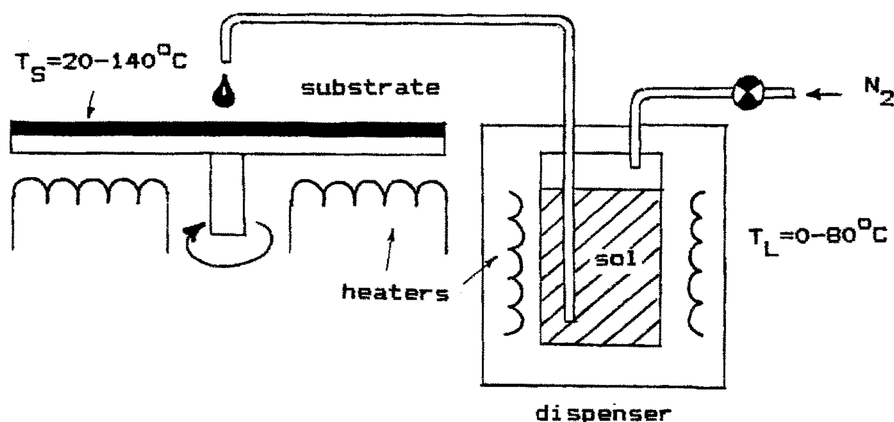

Fig. 3. Schematic representation of experimental equipment.

place in a relatively long time interval and the flow of highly aggregated molecules having non-newtonian behavior even at low shear rates occurs during some period of time. Moreover, a densification of the gel-like film at the edge of the substrate (after liquid outflow is ceased) may occur as a result of shear stress caused by centrifugal force. Both of these mechanisms (non-newtonian behaviour of liquid and shear stress densification of the gel-like film) lead to a thinning and a densification of the film at the edge of the substrate.

As a whole, the performed analysis of spin speed dependence of the sol-gel films may be considered as no more than a preliminary one. More wide and detailed investigation is needed, including the examination of sols with various polymer networks and solvents, study of initial sol rheology, careful consideration of gas phase convection, and also the production of a contour map for the whole wafer as it was demonstrated by Bornside et al. [21]. It is obvious that the uniformity of film thickness and microstructure is very important particularly for microelectronic applications, as it can lead to the change in elements sizes during lithography process.

4 Effect of Substrate Temperature and Temperature of Applied Solution on Sol-Gel Film Properties

4.1 Experimental Procedures

The special spin coater providing a possibility to change the substrate and solution temperatures has been created to carry out the experiment (see Fig. 3). The wafer holder was heated by an electric heater. Substrate temperature T_S was controlled by contact thermocouples before application and comprised $T_S =$ 20–140°C. The dispenser with coating liquid was placed into a special thermostat maintaining the liquid temperature T_L from room temperature to 80°C. For application at $T_L = 0$°C the dispenser was placed into a container with ice. The dosage of applied solution was 1 ml and was adjusted by the time of switching the gas pressure upon the dispenser in connection with the change of liquid viscosity with temperature.

The equivalent oxide concentration was 4 wt.% in these experiments. The other solution preparation conditions and wafer cleaning ones were consistent with those described in Section 3.1.

Film thicknesses and refractive indices were measured at the wafer center of as prepared films and after their heat treatment at 200, 400 and 700°C for 30 min in the air.

4.2 Film Thickness

The dependence of the film thickness h_f of silicate sol-gel films upon annealing temperature T_a at various temperatures of applied solution T_L and substrate temperature T_s is shown in Fig. 4. The increase in the substrate temperature as well as the solution temperature is observed to lead to the increase of the film thickness. The tendency is retained after film densification during the following treatment.

A number of principal temperaturedependent factors influencing the film thickness may be stand out analyzing Eq. (1): the density and viscosity of solution ρ_1

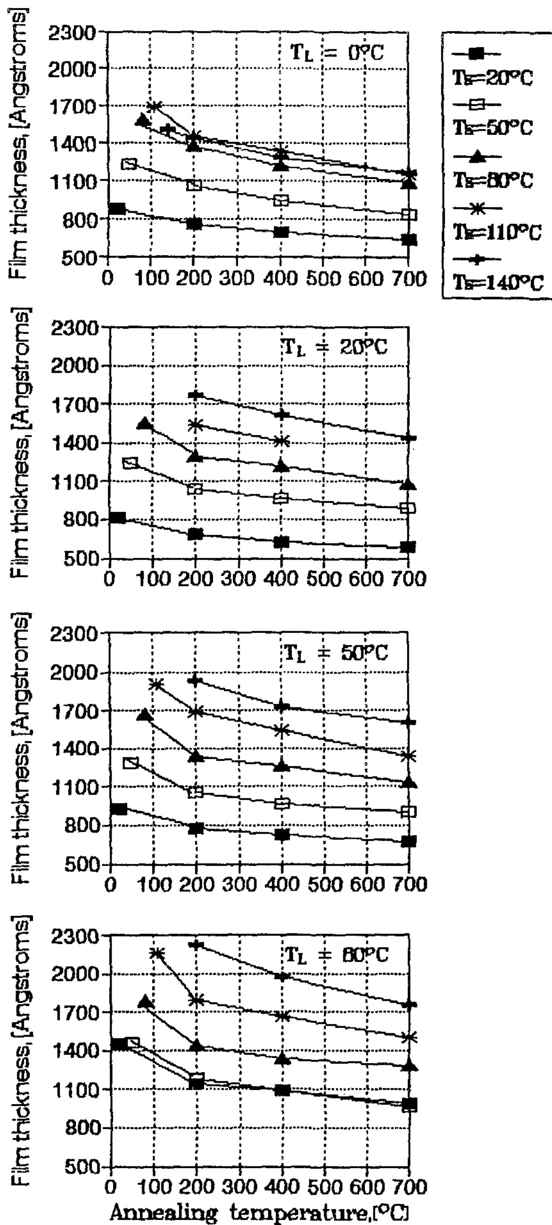

Fig. 4. The film thickness h_f of silicate sol-gel films as a function of annealing temperature T_a. The substrate temperature during spin coating T_s and the temperature of applied liquid T_L are taken as parameters.

and η_1^0, and evaporation rate which may be expressed in terms of the mass transfer coefficient k and the solvent vapour pressure p^*. The solution viscosity and the solvent vapour pressure have the most important exponential temperature dependences.

The change in viscosity with temperature in the first approximation may be expressed by Andrade equation [30]:

$$\eta_1 = A_1 \exp(B/T), \tag{7}$$

where A_1 is the constant dependent on the properties of liquid and weakly on temperature, B is the constant dependent on activation energy of molecules. Decrease of viscosity with temperature leads to the increase of the liquid flow flung off by centrifugal force and, consequently, to the decrease in the thickness of the film formed. In contrast to it, the increase of vapour pressure with temperature leads to the increase of the film thickness. The temperature dependence of vapour pressure can be approximated by the following equation [30]:

$$p^* = A_p \exp(-C/T), \tag{8}$$

where A_p is the constant dependent on solvent properties and weakly on the temperature, C is the constant nearly equal to the latent heat of evaporation.

Thus in accordance with Eqs. (1), (7), (8) the dependence of the $\ln h_f$ on the inverse temperature may be approximated by the line with the slope

$$\ln h_f \propto \frac{1}{3}\frac{(-C+B)}{T}. \tag{9}$$

For numerical estimation use the data for n-butanol. Approximating the experimental data on viscosity and vapour pressure for n-butanol in the range from 0 to 120°C [30] by Eqs. (7) and (8) we obtain B = 2299 K and C = 6549 K. Thus for n-butanol $\ln h_f \propto -1417/T$.

The dependence of $\ln h_f$ versus inverse substrate temperature and the temperature of applied liquid as a parameter is shown in the Fig. 5. To avoid an influence of film porosity we have used the thicknesses of the films after the heat treatment at T_a = 700°C, considering that this heat treatment is sufficient for film densification and $V_s \approx 1$ in Eq. (3). There exist three points on the plot in which $T_S = T_L(20, 50, 80°\text{C})$. The line approximating these points has the slope $\ln h_f \propto -1344/T$. In general, in terms of the made assumptions this value is close to the theoretical estimations for n-butanol. In the range of T_S = 20–80°C and T_L = 0–50°C the temperature of the deposited liquid do not sufficiently effect the film thickness, but at higher T_S the influence of T_L upon the thickness increases: the decrease in T_L leads to significant reduction of the film thickness (see Fig. 5). The latter may be caused by the heat exchange between the applied liquid and the substrate: for $T_L < T_S$ the applied solution cools the substrate leading to the decrease of

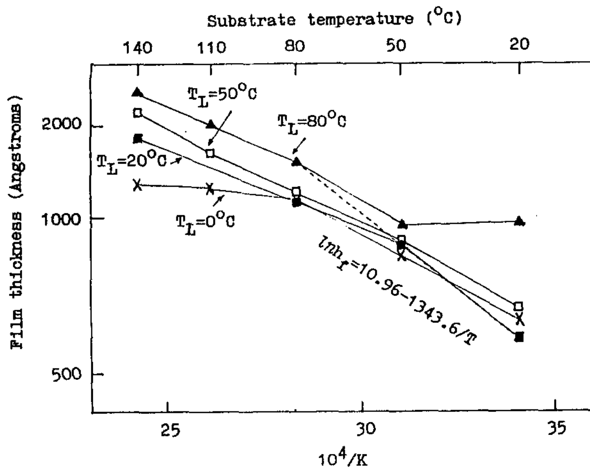

Fig. 5. The film thickness h_f of silicate sol-gel films (after drying at 700°C) versus substrate temperature during spin coating T_s, the temperature of applied liquid T_L being taken as a parameter.

the effective temperature of deposition process and, therefore, to the decrease of film thickness. Similarly, the deviation from linear dependence at $T_L = 80°\text{C}$ and $T_S = 20$–$50°\text{C}$ is associated with the increase of effective temperature of the process (upto approximately 60°C, see Fig. 5) due to the heat exchange between the liquid with higher temperature and the substrate.

4.3 Refractive Index and Shrinkage

The refractive index n_f and the film shrinkage (of as prepared films and after bake at 200°C) of silicate sol-gel films as a function of annealing temperature T_a at the different substrate temperatures T_S and the temperatures of applied liquid T_L are presented in the Figs. 6 and 7. Some of these data are collected in the Fig. 8 represented the dependencies of the refractive index (after the heat treatment at $T_a = 200°\text{C}$) as well as the film shrinkage (after the heat treatment at 200°C of as prepared films, and after further annealing of these films at 400°C) versus the substrate temperature during spin coating T_S (with T_L as a parameter).

The refractive index is fairly slowly changed with annealing temperature in spite of significant film shrinkage, particularly at the first drying stage (Figs. 6 and 7). The change in the substrate temperature as well as the liquid temperature have also low impact on the refractive index except of high values of T_S where it is somewhat increased that may be connected with a more dense film structure (Fig. 8a).

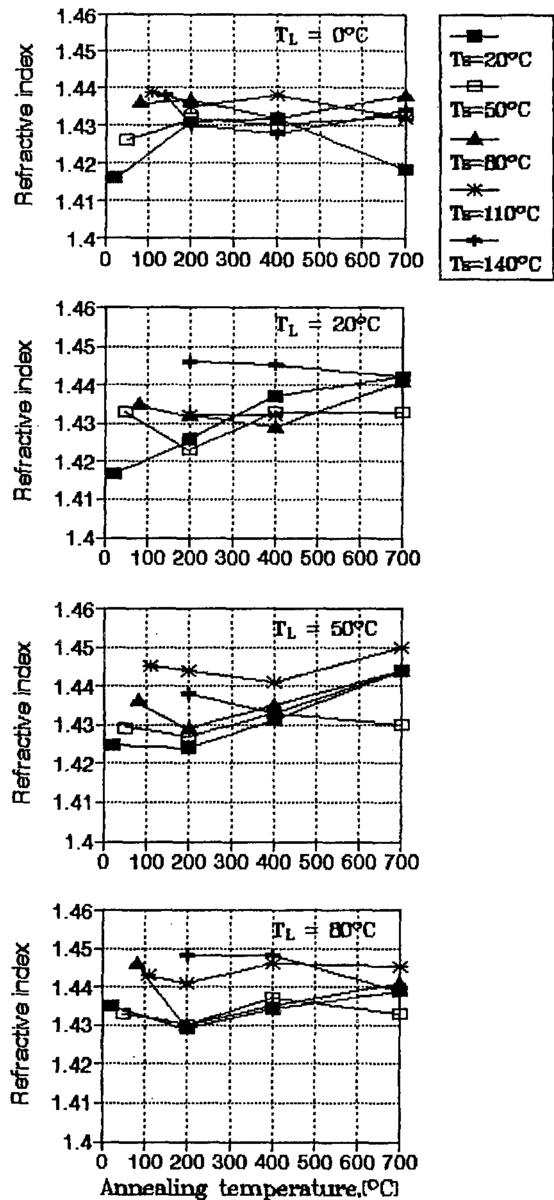

Fig. 6. The refractive index n_f of silicate sol-gel films as a function of annealing temperature T_a. The substrate temperature during spin coating T_s and the temperature of applied liquid T_L are taken as parameters.

The shrinkage of as prepared films after bake at 200°C varies weakly with T_s, but there is a tendency for a decrease at high values of T_s as the first drying stage occurs immediately during film application (Fig. 8b). It leads to densification of as prepared films and correspondent decrease of their further shrinkage. The rise in the temperature of applied liquid T_L causes, contrastingly, more pronounced increase of film shrinkage. The reason is that the solution temperature has its main

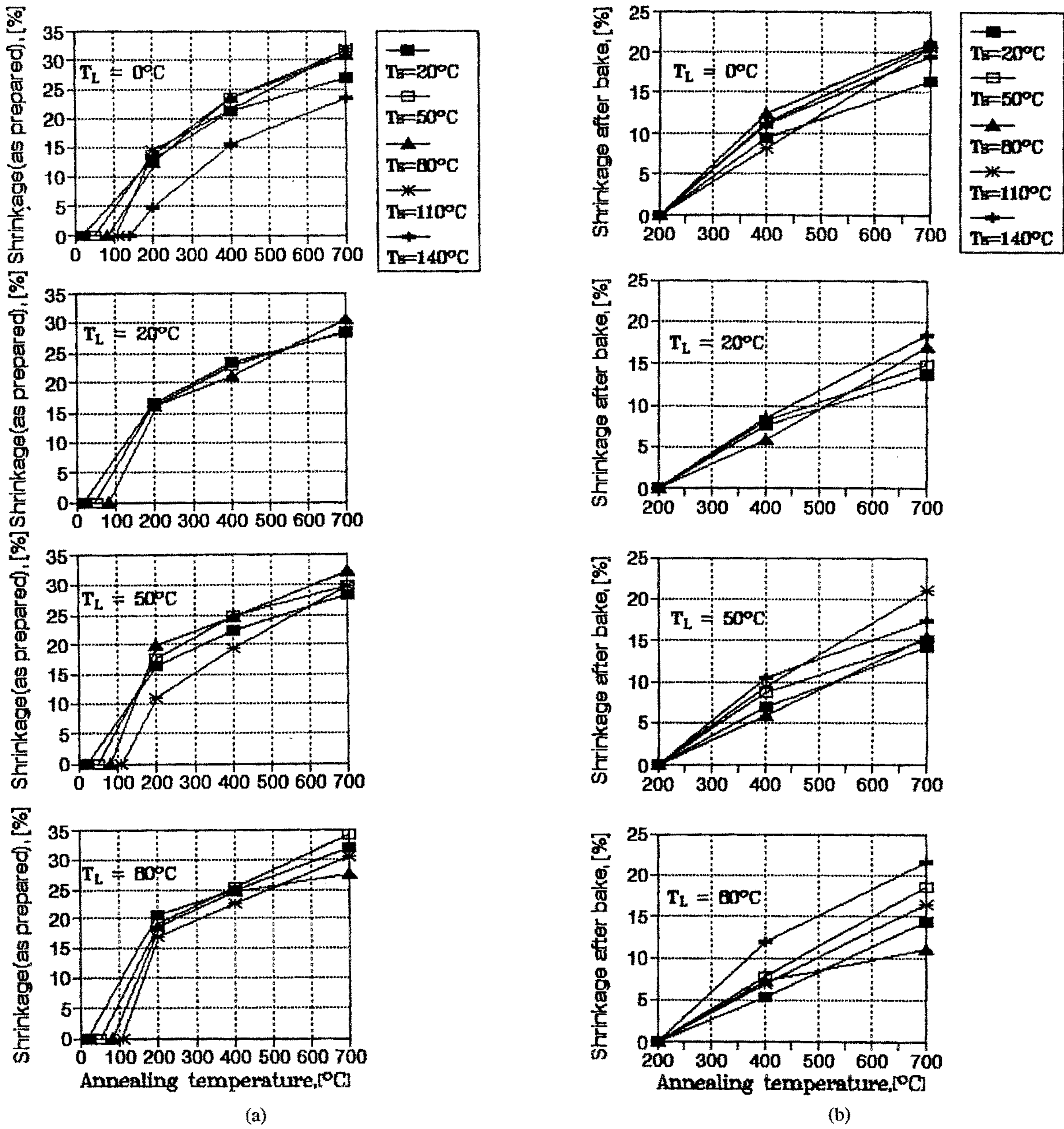

Fig. 7. The film shrinkage of silicate sol-gel films as a function of annealing temperature.
(a) The shrinkage of as prepared films; (b) the shrinkage after bake at 200°C.

influence at the spin-off stage of spin coating process, but less at the following ones due to heat exchange with the substrate as it was discussed previously. For example, if $T_L > T_S$ an increase of the effective process temperature at the first stage of spin coating leads to formation of thicker film with a weakly branched network, and therefore with a higher value of shrinkage during further heat treatment.

The shrinkage during further heat treatment at 400°C (Fig. 8(c)) remains practically constant for all substrate temperatures despite the significant rise in film thickness (the increase of the film thickness of sol-gel films, e.g., if concentration increases, leads typically to less dense films with higher shrinkage (e.g., [31]). Thus, in contrast to other methods of film thickness increase, the increase in T_s does not cause the rise in film porosity.

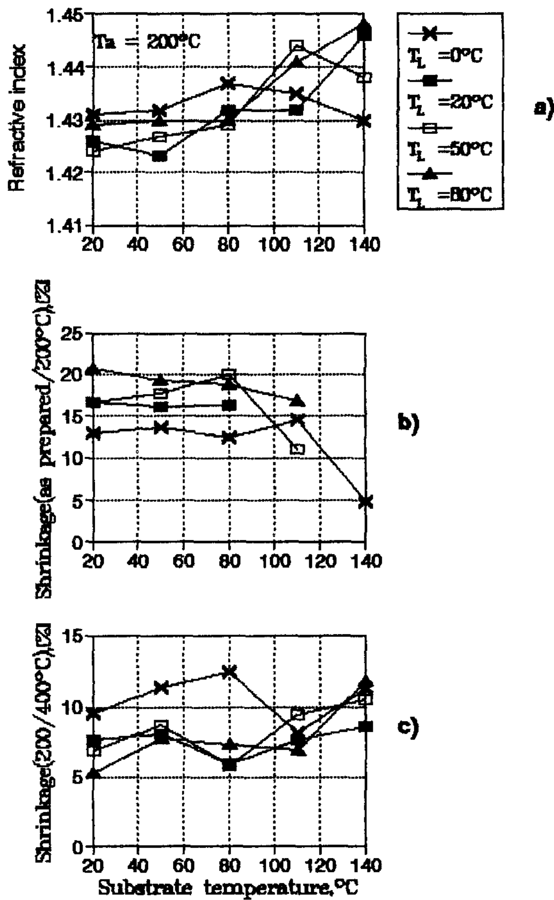

Fig. 8. The refractive index ($T_a = 200°C$) (a), the film shrinkage (as prepared/200°C) (b) and the film shrinkage (200°C/400°C) (c) of silicate sol-gel films versus the substrate temperature during spin coating T_s, the temperature of applied liquid T_L being taken as a parameter.

The possible reason of this may be a temperature gradient perpendicularly to the film surface acting during spin coating process. The drying process in this case occurs from bottom to top of the film. This prevents the developing of the surface skin layer during spin coating process (which may hinders solvent evaporation and may provokes aggregation of polymer species) and result in compact package of polymer species.

5 Conclusions

Spin coating process appears to be the most important practical technique for thin film formation from liquid precursors in microelectronics and some others industries. The examination of the spin coating process of sol-gel films includes the centrifugal driving force dynamics, viscous polymer rheology, solvent evaporation dynamics, and transformation of film porous microstructure.

The obtained experimental dependence of thickness of sol-gel silicate films on spin speed $h_f \propto \omega^{-\lambda}$ has the slope $\lambda = 0.6$, that differs from the Meyerhofer's approximation ($\lambda = 0.5$). This deviation may be caused by different reasons, such as the change in the film porosity, the solvent evaporation behaviour, and the non-newtonian rheology of deposited solution. Unfortunately, the refractive index of silicate films does not adequately determine film porosity because of high hydroxyl content in the films, and it is fairly hard to determine its real contribution in λ. The other reasons of deviation of λ from theoretical value may be connected both with the solvent evaporation behaviour, namely, with formation of the so-called skin layer with low solvent concentration at the free surface and low binary diffusivity that hinders the free solvent evaporation, and also with the non-newtonian rheology of deposited solution. The latter leads to observed radial nonuniformity of the films (the film thickness decreases from the center to the edge of the wafer). Closer examination of mechanisms of sol-gel films formation requires more wide and combined investigations. It is of not only a scientific importance, but also of a vital practical one particularly for microelectronic applications of such films (the thickness and microstructure uniformity of sol-gel films are critical issues in lithography and etching processes).

A rise in the substrate temperature as well as in the deposited liquid temperature leads to formation of thicker films. The temperature dependence of films thickness is mainly determined by the change in solvent vapour pressure with consideration for the change in liquid viscosity. To a first approximation the dependence of $\ln h_f$ on the inverse temperature is linear with the slope

$$\ln h_f \propto \frac{1}{3}(-C + B)/T,$$

where C and B are the powers in temperature dependencies of solvent vapour pressure and liquid viscosity, correspondingly. Deviations from linear dependence at distinct temperatures of the substrate and the applied liquid are associated with the change in effective temperature of the coating process due to heat exchange between the liquid and the substrate.

In contrast to other methods of film thickness increase (e.g., by concentration) the increase in the substrate temperature does not cause the rise in film porosity (film shrinkage remains constant).

Acknowledgment

The research described in this work was made possible in part by Grant N MRQ 300 from the International Science Foundation.

References

1. C.J. Brinker and G.W. Scherer, *Sol-Gel Science: The Physics and Chemistry of Sol-Gel Processing* (Academic Press, San Diego, CA, 1990).
2. *Sol-Gel Techology for Thin Films, Fibers, Preforms, Electronics, and Speciality Shapes*, edited by L.C. Klein (Noyes, Park Ridge, N.J., 1988).
3. L.D. Molnar, Semiconductor International **12**, 92 (1989).
4. J.F. Scott, C.A. Paz De Araujo, and L.D. McMillan, Condensed Matter News **1**, 16 (1992).
5. A.S. Sigov, K.A. Vorotilov, A.S. Valeev, and M.I. Yanovskaya, Journal of Sol-Gel Science and Technology **2**, 563 (1994).
6. *Precision Cleaning and Meniscus Coating System*, Specialty Coating Systems, Inc.
7. L.D. McMillan, C.A. Paz De Araujo, T. Roberts, J. Cuchiaro, M.C. Scott, and J.F. Scott, Integrated Ferroelectrics **2**, 351 (1992).
8. C.J. Brinker, A.J. Hurd, G.C. Frye, K.J. Ward, and C.S. Ashley, Journal of Non-Cryst. Solids **121**, 294 (1990).
9. I. Strawbridge and P.F. James, Journal of Non-Cryst. Solids **86**, 381 (1986).
10. D.E. Bornside, C.W. Macosko, and L.E. Scriven, Journal of Imagine Technology **13**, 122 (1987).
11. A.G. Emslie, F.T. Bonner, and L.G. Peck, Journal of Applied Physics **29**, 858 (1958).
12. A. Acrivos, M.J. Shah, and E.E. Petersen, Journal of Applied Physics **31**, 963 (1960).
13. D. Meyerhofer, Journal of Applied Physics **49**, 3993 (1978).
14. W.W. Flack, D.S. Soong, A.T. Bell, and D.W. Hess, Journal of Applied Physics **56**, 1199 (1984).
15. S.A. Jenekhe and S.B. Schuldt, Ind. Eng. Chem. Fundam. **23**, 432 (1984); S.A. Jenekhe, Ind. Eng. Chem. Fundam. **23**, 425 (1984).
16. C.J. Lawrence, Phys. Fluids **31**, 2786 (1988).
17. D.E. Bornside, C.W. Macosko, and L.E. Scriven, Journal of Applied Physics **66**, 5185 (1989).
18. S. Shimoji, Journal of Applied Physics **66**, 2712 (1989).
19. P.C. Sukanek, Journal of Electrochemical Society **138**, 1712 (1991).
20. D.E. Bornside, C.W. Macosko, and L.E. Scriven, Journal of Electrochemical Society **138**, 317 (1991).
21. D.E. Bornside, R.A. Brown, P.W. Ackmann, J.R. Frank, A.A. Tryba, and F.T. Geyling, Journal of Applied Physics **73**, 585 (1993).
22. L.E. Stillwagon, R.G. Larson, and G.N. Taylor J. Electrochem. Soc. **134**, 2030 (1987).
23. P.C. Sukanek, J. Electrochem. Soc. **136**, 3019 (1989).
24. D.E. Bornside, J. Electrochem. Soc. **137**, 2589 (1990).
25. C.J. Brinker, A.J. Hurd, G.C. Frye, K.J. Ward, and C.S. Ashley, J. Non-Cryst. Solids **121**, 294 (1990).
26. K.A. Vorotilov, V.A. Vasiljev, M.V. Sobolevsky, V.I. Petrovsky, and N.I. Afanasjeva, Thin Solid Films, submitted for publication.
27. D.J. Taylor and B.D. Fabes, J. Non-Cryst. Solids **147&148**, 457 (1992).
28. V.K. Grigor'ev, V.I. Petrovsky, and I.A. Shapova, Izmeritelnaya Technika **1**, 15 (1991) (in Russian).
29. S. Wu, J. Electrochem. Soc. **130**, 199 (1983).
30. R.C. Reid, J.M. Pransnitz, and T.K. Sherwood, *The Properties of Gases and Liquids* (McGraw-Hill, NY, 1977; in Russian translation: Leningrad, 1982).
31. K.A. Vorotilov, E.V. Orlova, and V.I. Petrovsky, Thin Solid Films **209**, 188 (1992).